Nuclear Physics A368 (1981) 445–476

THE QUASIPARTICLE INTERACTION, A SHIELD OF NUCLEAR MATTER AGAINST PION CONDENSATION

W.H. DICKHOFF

Natuurkundig Laboratorium, Vrije Universiteit, Amsterdam, Netherlands

AMAND FAESSLER

Institut für Theoretische Physik, Universität Tübingen, D-7400 Tübingen, W.-Germany

J. MEYER-TER-VEHN

Projektgruppe für Laserforschung, Max Planck Gesellschaft, D-8046 Garching, W.-Germany

and

H. MÜTHER

Institut für Theoretische Physik, Universität Tübingen, D-7400 Tübingen, W.-Germany

Received 30 March 1981

Abstract: A microscopic calculation is presented for the quasiparticle interaction in nuclear matter. As a starting point a Brueckener G-matrix is used, which is derived from realistic potentials (Reid soft core, HM2Δ). Keeping the full complexity of this interaction, the excitation modes for the different spin–isospin channels are evaluated. The effects of isobar excitation [$\Delta(3,3)$] are also taken into account. The exchange of the corresponding phonons is added to the bare G-matrix and the influence of this so-called crossed channel renormalization on the interaction of quasiparticles at the Fermi surface is discussed. This renormalization of the particle–hole interaction increases drastically the critical density for pion condensation in nuclear matter.

1. Introduction

During the last few years a large number of theoretical investigations have been made to study the question under which conditions (density ρ, temperature T) a phase transition to a pion condensate may occur in nuclear matter or neutron stars [1–3]). Originally this question was raised by the proposals of Migdal [4]) and independently by Sawyer and Scalapino [5]). More recently, the discussion of the possible existence of so-called "precursor phenomena" has even increased the interest in this phase transition. These "precursor phenomena", which have been discussed e.g. in the theoretical analysis of inelastic proton scattering by Toki and Weise [6]) and for the (e, e') isovector magnetic scattering by Delorme *et al.* [7]), can be understood as an indication for the proximity of pion condensation already in nuclear systems at normal densities.

The theoretical determination of the threshold for pion condensation depends crucially on the excitation mechanism of Δ-isobar states and the residual nuclear correlations as pointed out by Bäckman and Weise [3,8]) and by Brown and Weise [1]). Here, residual nuclear correlations stand for the interaction of particle–hole states carrying the quantum numbers of the pion, except the direct one-pion exchange part. Typically, this residual particle–hole interaction is represented in momentum space by a constant, which does not depend on the momenta of the interacting particle–hole states. In the limit of particle–hole states of total momentum $k = 0$, this constant is related to the parameter G_0' in the Landau-Migdal parametrization (definition see below in subsect. 2.1) of the quasiparticle interaction. Therefore it has often been determined from the empirical value of G_0' which has been adjusted by Speth *et al.* [9]) and Meyer-ter-Vehn [10]) in microscopic calculations of low-lying excited states of finite nuclei. Now the question is, is it justified to use the strength of the residual interaction also for the calculation of the threshold for pion condensation, although typically particle–hole states of large momenta ($k \approx 2m_\pi$) are involved, and also systems of larger density have to be considered.

There have been attempts to derive the effective interaction strength from the Brueckner G-matrix [8,11,12]), which is an effective nucleon–nucleon (NN) interaction in nuclear matter, microscopically derived from a realistic free NN interaction. Indeed, those investigations show that the resulting interaction strength does not vary rapidly as a function of the particle–hole momentum k or the nuclear density ρ [ref. [12])]. This seems to support the procedure to determine the nuclear correlations, to be considered in the calculation of the threshold for pion condensation, from the empirical Landau parameter G_0', mentioned above.

The approximation to describe the residual particle–hole interaction by the Brueckner G-matrix, only, could be too simple and therefore the conclusion of a constant G_0' which does not depend on momentum and density might be premature. This is supported by the following intuitive argument: A part of the residual interaction originates from the exchange term of the one-pion-exchange potential as displayed in fig. 1a. If one now considers a nuclear system which is close to the

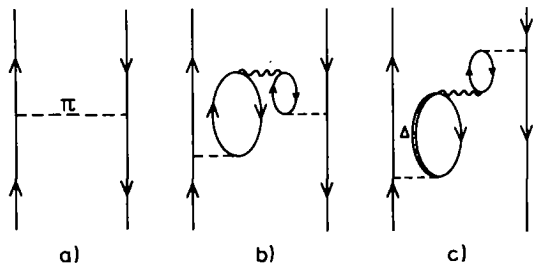

Fig. 1. Exchange term of the one-pion-exchange potential for the particle–hole interaction (a) and contributions to its modification in the nuclear medium (b) and (c).

threshold for pion condensation, the propagation of the pion will be strongly affected by the strong coupling of the pion to the corresponding excitation mode of the nuclear system. This means the series of diagrams, which is characterized by the 2 examples displayed in figs. 1b and 1c, should lead to a considerable renormalization of the residual interaction, which may show up in a drastic modification of the effective strength, if one approaches the critical point.

It is the aim of the present paper to investigate the renormalization of the particle–hole interaction due to terms as displayed in figs. 1b and 1c for nuclear matter of normal density ($k_F = 1.4\,\mathrm{fm}^{-1}$). Since the isobar excitations play an essential role in the calculation of the pion self-energy, which is needed to determine the threshold condition for pion condensation, the Δ-isobar excitations are also considered in calculating the renormalization of the residual interaction (see fig. 1c). Also the renormalization due to intermediate particle–hole states with quantum numbers different from the pion are taken into account.

The general idea behind the present approach is the following: If we want to describe a collective particle–hole state, we also allow the particle and hole states to exchange such a collective phonon in the crossed channel (see figs. 1b, c). This can lead to a strong renormalization of the residual interaction in the particle–hole channel. Here we would like to point out that for general physical systems collective features are enhanced with increasing density and therefore these renormalization terms in the expansion of the effective interaction might be dominant. The next step would be to take such a renormalization already into account for calculating the collective phonons in the crossed channel etc. This iterative approach corresponds to the induced interaction approach discussed by Babu and Brown [13]) for liquid ^{3}He. For nuclear matter these ideas have been applied by Sjöberg [14]). Restricting to pure nucleonic excitations the induced interaction approach yields a quasiparticle interaction which fulfills the Pauli principle and therefore yields the corresponding sum rules [13,15]).

In the present work we consider the induced interaction only in lowest order (see above). In contrast to refs. [13,14]), however, we solve the problem keeping the full complexity of the interaction, which is dependent on spin, isospin, energy and three momentum variables. Also isobar excitations are taken into account. As the basic building blocks for the crossed channel renormalization we use the Brueckner G-matrix and transition potentials to describe isobar excitations, which take into account the effects of short-range correlations analogous to the G-matrix. At present we do not consider any renormalization of the effective interaction which is not contained in the crossed channel renormalization. Such terms arise e.g. in the approach of Brown [16]) and Bäckman [17]), who obtain an approximation for the quasiparticle interaction by functional differentiation of the Brueckner–Hartree–Fock energy with respect to the quasiparticle distribution function. We use two different realistic NN interactions, which both fit the experimental NN data, the phenomenological Reid soft-core potential [18]) and the extended form of a

one-boson-exchange potential HM2Δ [ref. [19])] which has a much weaker tensor component than the Reid soft-core potential.

We start in subsect. 2.1 by giving a summary of the necessary formal many-body theory to arrive at the quasiparticle interaction. In addition we recapitulate the definition of the Landau parameters as well as give some useful relations which connect some of these parameters to some of the physical properties of the system. In subsect. 2.2 we describe the calculation of the G-matrix. Next we discuss the crossed channel integral equation and develop it into a form which is suitable for numerical calculation. In subsect. 2.3 we develop the formalism to include the isobars in the calculation. Sect. 3 is devoted to a discussion of the results while some conclusions are drawn in the final sect. 4.

2. The cross-channel renormalization

2.1. THE QUASIPARTICLE INTERACTION

This section contains a summary of some formal aspects of many-body theory. Most of these aspects have been discussed already in the literature [20]). Nevertheless, we think that this summary might be helpful for the reader, to get a formal framework for the investigations discussed in this paper. In addition, we will define the notation to be used in the following sections. We will consider the four-point vertex function Γ [see eq. (2.1)], which describes the complete interaction of two quasiparticles, in the limit that the four-momentum transfer in the Landau channel goes to zero [see eq. (2.2)]. That part of Γ, which is irreducible with respect to intermediate particle–hole states with energy and momentum on the Fermi surface, is denoted by Γ^0 [see eq. (2.4)] and can be identified with the so-called quasiparticle interaction in the Landau limit [see eq. (2.6)]. Furthermore we will present the parametrization of this quasiparticle interaction in terms of Landau parameters.

In momentum space, the two-particle Green function which describes the propagation of two quasiparticles in an infinite homogeneous many-body system, can be written

$$
\begin{aligned}
&g^{\mathrm{II}}_{\alpha\beta,\gamma\delta}(p_1, p_2, p_3, p_4) \\
&= \delta_{\alpha\gamma} g(p_1)\delta_{\beta\delta} g(p_2)\delta^{(4)}(p_1 - p_3)(2\pi)^4 - \delta_{\alpha\delta} g(p_1)\delta_{\beta\gamma} g(p_2)\delta^{(4)}(p_2 - p_3)(2\pi)^4 \\
&\quad + i g(p_1) g(p_2) g(p_2) g(p_4) \Gamma_{\alpha\beta,\gamma\delta}(p_1, p_2, p_3, p_4)\,, \qquad (2.1)
\end{aligned}
$$

where g^{II} and Γ do not contain the δ-function due to four-momentum conservation. Here g denotes the single-particle Green function, p_i are four-momenta and $\alpha, \beta, \gamma, \delta$ are spin-isospin indices. Γ stands for the fully reducible four-point vertex function. This vertex function contains all possible interactions and intermediate propagation which connect the four external four-momenta. The part which

describes free propagation is considered explicitly in eq. (2.1) and therefore should not be contained in Γ. For further discussion we make use of four-momentum conservation and define the momentum variables of Γ by $p_1 = p + \frac{1}{2}k$, $p_2 = p' - \frac{1}{2}k$, $p_3 = p' + \frac{1}{2}k$ and $p_4 = p - \frac{1}{2}k$ (see fig. 2). The simplest diagram contained in Γ is just the bare nucleon–nucleon interaction V. To calculate Γ one must sum the entire series of perturbation theory. As has been discussed by Landau [20]) one can separate out the parts having a singularity at $p = p'$, by noting that these singularities are due to diagrams that have parallel pairs of lines with nearly equal values of four-momentum (in the limit $p \to p'$), like the second diagram on the right-hand side in fig. 2. If we now

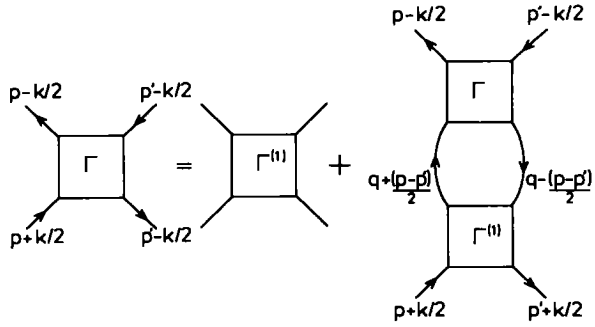

Fig. 2. Integral equation for Γ where we have singled out that part, $\Gamma^{(1)}$ which has no singularities for $p \to p'$. The singularities are contained in the second diagram on the right-hand side where the intermediate state contains a parallel pair of lines with nearly equal four-momenta in the limit $p \to p'$.

separate from Γ the diagrams which do not have this singularity and denote this part by $\Gamma^{(1)}$. We can clearly sum the entire series by solving the integral equation

$$\Gamma_{\alpha\beta,\gamma\delta}(\tfrac{1}{2}(p+p'+k), \tfrac{1}{2}(p+p'-k); p-p') = \Gamma^{(1)}_{\alpha\beta,\gamma\delta}(p+\tfrac{1}{2}k, p-\tfrac{1}{2}k)$$
$$+ \int \frac{d^4q}{i(2\pi)^4} \Gamma^{(1)}_{\alpha\varepsilon,\gamma\eta}(p+\tfrac{1}{2}k, q) g(q+\tfrac{1}{2}(p-p'))$$
$$\times g(q-\tfrac{1}{2}(p-p')) \Gamma_{\eta\beta,\varepsilon\delta}(q, \tfrac{1}{2}(p+p'-k); p-p')), \qquad (2.2)$$

which is shown graphically in fig. 2. $\Gamma^{(1)}$ is sometimes called the irreducible particle–hole interaction with no "$p-p'$ cuts". The diagrams, reading from the bottom to the top, illustrate the iteration in the Landau channel. We arrange the momentum variables in eq. (2.2) in the order incoming, outgoing relative four-momentum and for Γ also the total four-momentum $p-p'$ which is conserved everywhere. Since $\Gamma^{(1)}$ has no singularity for $p \to p'$ we have taken this limit.

Repeated spin–isospin indices implies summation. The product of the two single-particle Green functions contains the singularity which can be isolated, giving in the limit $p \to p'$

$$g(q+\tfrac{1}{2}(p-p'))g(q-\tfrac{1}{2}(p-p'))$$
$$\Rightarrow 2\pi i z^2_{|q|} \frac{(\boldsymbol{p}-\boldsymbol{p}')\cdot\hat{\boldsymbol{q}}}{p_0-p_0'-(\boldsymbol{p}-\boldsymbol{p}')\cdot\boldsymbol{q}/m^*}\,\delta(\varepsilon_F-q_0)\delta(k_F-|\boldsymbol{q}|)+g^2(q)\,, \qquad (2.3)$$

where we denote the time component of the four-momenta with a subscript 0, ε_F and k_F are the Fermi energy and momentum, respectively, $z_{|q|}$ is the single-particle strength and m^* the effective mass of the nucleons at the Fermi surface. Clearly the pole part of eq. (2.3) depends on the way in which $\boldsymbol{p} \to \boldsymbol{p}'$ and $p_0 \to p_0'$. Letting first $\boldsymbol{p} \to \boldsymbol{p}'$ and then $p_0 \to p_0'$, the first term on the r.h.s. of eq. (2.3) vanishes. This means that in this limit the vertex function Γ, which we denote by Γ^0, can be written as

$$\Gamma^0_{\alpha\beta,\gamma\delta}(p+\tfrac{1}{2}k, p-\tfrac{1}{2}k) = \Gamma^{(1)}_{\alpha\beta,\gamma\delta}(p+\tfrac{1}{2}k, p-\tfrac{1}{2}k)$$
$$+\int \frac{d^4q}{i(2\pi)^4}\,\Gamma^{(1)}_{\alpha\varepsilon,\gamma\eta}(p+\tfrac{1}{2}k, q)g^2(q)\Gamma^0_{\eta\beta,\varepsilon\delta}(q, p-\tfrac{1}{2}k)\,. \qquad (2.4)$$

This shows that the vertex function in this limit, Γ^0, does not contain any intermediate particle–hole states where both particle and hole are at the Fermi surface, since the propagation of these states is represented by the first term of eq. (2.3) which vanishes in this limit. In other words, this means that Γ^0 is irreducible with respect to those particle–hole states. An example of a reducible diagram which is not contained in Γ^0 is given in fig. 3a (with $p = p'$). The exchange term of this diagram can be obtained by exchanging e.g. the outgoing lines and is displayed in fig. 3b. It is clear that diagram 3b is irreducible with respect to the particle–hole states discussed above and therefore is contained in Γ^0. This shows, that Γ^0 is not antisymmetric whereas the full vertex function Γ is antisymmetric. The full vertex function Γ can be expressed in

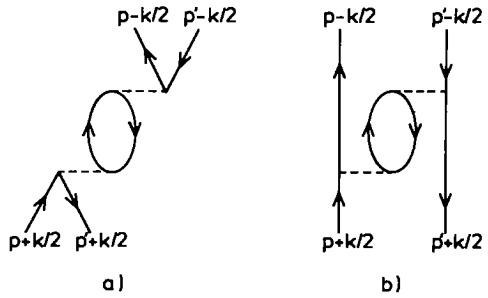

Fig. 3. Diagrams with intermediate particle–hole states as discussed in the text. Note that diagram (a) contains a pole term in the Landau channel ($p \to p'$) whereas diagram (b) contains a pole in the crossed channel ($k \to 0$).

terms of Γ^0 by eliminating $\Gamma^{(1)}$ from eqs. (2.2) and (2.4).

$$\Gamma_{\alpha\beta,\gamma\delta}(\tfrac{1}{2}(p+p'+k),\tfrac{1}{2}(p+p'-k);p-p')$$
$$=\Gamma^0_{\alpha\beta,\gamma\delta}(p+\tfrac{1}{2}k,p-\tfrac{1}{2}k)+\int\frac{d\Omega_q}{4\pi}\frac{z^2k_F^2}{2\pi^2}\Gamma^0_{\alpha\varepsilon,\gamma\eta}(p+\tfrac{1}{2}k,q)$$
$$\times\frac{(\boldsymbol{p}-\boldsymbol{p}')\cdot\hat{\boldsymbol{q}}}{p_0-p_0'-(\boldsymbol{p}-\boldsymbol{p}')\cdot\boldsymbol{q}/m^*}\Gamma_{\eta\beta,\varepsilon\delta}(q,\tfrac{1}{2}(p+p'-k);p-p')\,. \tag{2.5}$$

We see that the intermediate particle–hole states with particle and hole at the Fermi surface, which were cut out in Γ^0 are treated explicitly in eq. (2.5). We stress that the four-momenta p and k in eq. (2.5) are still completely free, only the intermediate four-momentum q is restricted to the Fermi surface ($q_0=\varepsilon_F$, $|\boldsymbol{q}|=k_F$). This implies for example that the first term on the r.h.s. of eq. (2.5) still contains singularities when the four-momentum k in the crossed channel goes to zero. An example of such an intermediate particle–hole state in the crossed channel is displayed in fig. 3b ($p=p'$). However these singularities disappear in the Landau limit when we put $p+\frac{1}{2}k$ and $p-\frac{1}{2}k$ on the Fermi surface ($p_0\pm k_0/2=\varepsilon_F$ and $|\boldsymbol{p}\pm\frac{1}{2}\boldsymbol{k}|=k_F$). In this case k_0 is strictly zero and therefore terms which may lead to singularities in the crossed channel analogous to the pole term in eq. (2.3) are well behaved. Denoting for the moment $\boldsymbol{p}+\frac{1}{2}\boldsymbol{k}$ by $\boldsymbol{p}_1$ and $\boldsymbol{p}-\frac{1}{2}\boldsymbol{k}$ by $\boldsymbol{p}_2$ we arrive at the following definition of the quasiparticle interaction

$$\mathcal{F}_{\alpha\beta,\gamma\delta}(\boldsymbol{p}_1,\boldsymbol{p}_2)\equiv z^2\Gamma^0_{\alpha\beta,\gamma\delta}(\boldsymbol{p}_1,\boldsymbol{p}_2)\,. \tag{2.6}$$

This quasiparticle interaction was first introduced by Landau in his work on the theory of the Fermi liquid [20,21]). It was later generalized by Migdal to include the isospin degrees of freedom for nuclear matter [22]). Since Migdal considered only central interactions, it was modified by Dabrowski and Haensel [23]) to deal with the tensor component of the nuclear force. In this form the quasiparticle interaction in nuclear matter is written as

$$\mathcal{F}(\boldsymbol{p}_1,\boldsymbol{p}_2)=f(\boldsymbol{p}_1,\boldsymbol{p}_2)+f'(\boldsymbol{p}_1,\boldsymbol{p}_2)\boldsymbol{\tau}_1\cdot\boldsymbol{\tau}_2+g(\boldsymbol{p}_1,\boldsymbol{p}_2)\boldsymbol{\sigma}_1\cdot\boldsymbol{\sigma}_2+g'(\boldsymbol{p}_1,\boldsymbol{p}_2)\boldsymbol{\sigma}_1\cdot\boldsymbol{\sigma}_2\boldsymbol{\tau}_1\cdot\boldsymbol{\tau}_2$$
$$+\frac{q^2}{k_F^2}h(\boldsymbol{\rho}_1,\boldsymbol{\rho}_2)S_{12}(\hat{\boldsymbol{q}})+\frac{q^2}{k_F^2}h'(\boldsymbol{\rho}_1,\boldsymbol{\rho}_2)S_{12}(\hat{\boldsymbol{q}})\boldsymbol{\tau}_1\cdot\boldsymbol{\tau}_2\,, \tag{2.7}$$

where $\boldsymbol{q}=\frac{1}{2}(\boldsymbol{p}_1-\boldsymbol{p}_2)$ with $\boldsymbol{p}_1$ and $\boldsymbol{p}_2$ on the Fermi surface (k_F) and

$$S_{12}(\hat{\boldsymbol{q}})=3\boldsymbol{\sigma}_1\cdot\hat{\boldsymbol{q}}\boldsymbol{\sigma}_2\cdot\hat{\boldsymbol{q}}-\boldsymbol{\sigma}_1\cdot\boldsymbol{\sigma}_2\,. \tag{2.8}$$

The connection of eq. (2.7) to $\mathcal{F}_{\alpha\beta\gamma\delta}$ is the following, the pair α, γ corresponds to $\boldsymbol{p}_1$ and $\boldsymbol{\sigma}_1$, $\boldsymbol{\tau}_1$ and likewise β, δ to $\boldsymbol{p}_2$ and $\boldsymbol{\sigma}_2$, $\boldsymbol{\tau}_2$. Since the quasiparticle interaction $\mathcal{F}$ depends only on the angle θ_L (L for Landau) between $\boldsymbol{p}_1$ and $\boldsymbol{p}_2$ it is customary to

make an expansion of the six amplitudes in terms of Legendre polynomials, for example

$$N_0 f(p_1, p_2) = \sum_l F_l P_l(\cos\theta_L)\,, \tag{2.9}$$

where

$$N_0 = 2m^* k_F/\pi^2 \tag{2.10}$$

is the density of states per unit energy at the Fermi surface per unit volume. The dimensionless parameters F_l, F_l', G_l etc. are called Landau parameters. The effective mass m^* at the Fermi surface in eq. (2.10) enters also in the derivation of the quasiparticle interaction. It can be calculated from the Landau parameter F_1

$$m^*/m = 1 + \tfrac{1}{3}F_1 \tag{2.11}$$

as shown by Landau [21]). Note that in eqs. (2.3) and (2.5) m^* is defined according to

$$k/m^* = \left.\frac{d\varepsilon_k}{dk}\right|_{k=k_F}, \tag{2.12}$$

where ε_k is the single-particle energy which is related to the kinetic energy T_k and the mass operator $M(k, E)$ by

$$\varepsilon_k = T_k = M(k, \varepsilon_k)\,. \tag{2.13}$$

Two other Landau parameters have a direct relationship with the properties of the system [22]). F_0 is related to the compressibility K

$$K = 6\frac{k_F^2}{2m^*}(1+F_0)\,, \tag{2.14}$$

and F_0' is related to the symmetry energy β

$$\beta = \frac{1}{3}\frac{k_F^2}{2m^*}(1+F_0')\,. \tag{2.15}$$

Finally, it is also possible to obtain two sum rules [24]) which put a restraint on the Landau parameters,

$$\sum_l (B_l + B_l' + C_l + C_l') = 0\,, \tag{2.16a}$$

$$\sum_l (B_l - 3B_l' - 3C_l + 9C_l') = 0\,, \tag{2.16b}$$

where for example

$$B_l = \frac{F_l}{2l+1}, \tag{2.17}$$

and a similar relation holds for B_l' and F_l'. The C_l and C_l' parameters have a more complicated connection to the Landau parameters, these relations are given explicitly in ref. [24]). These sum rules originate from the fact that the total vertex function Γ is antisymmetric. From eq. (2.5) we see that Γ calculated in a certain approximation is only antisymmetric if Γ^0 contains the exchange terms which correspond to the iteration in eq. (2.5).

2.2. MICROSCOPIC CALCULATION OF THE LANDAU PARAMETERS IN NUCLEAR MATTER

A microscopic calculation of the Landau parameters has to start with the bare nucleon–nucleon interaction V. We require V to describe the two-nucleon data and in that sense V is called realistic. In this investigation we will consider two different nucleon–nucleon interactions. The first one is the Reid soft-core potential [18]) supplemented in higher partial waves ($J > 2$) by an OBE potential. The other one is a more modern meson exchange potential called HM2Δ which is the HM2+Δ550 of ref. [19]). The main differences between these potentials are the much stronger tensor force of the Reid as compared to the HM2Δ and the explicit consideration of isobar degrees of freedom in the HM2Δ. Throughout this paper we will pay attention to possible similarities and differences between these potentials when they are introduced into the many-body system.

A very prominent feature of the bare nucleon–nucleon interaction is the strong repulsion at short distances. This means that it makes no sense to consider a perturbation expansion in terms of the bare nucleon–nucleon interaction. A way to overcome this difficulty is to make a partial summation of those terms in the perturbation series which represent any number of interactions V between a pair of nucleons. This procedure leads to a well-behaved effective interaction, the so-called Brueckner G-matrix. We will use the G-matrix as a starting point for calculations of the Landau parameters. To obtain the G-matrix for nuclear matter, we have solved the Bethe–Goldstone equation in momentum space using the matrix inversion technique as it is described in ref. [25]). The effective mass spectrum was used for the hole energies

$$\varepsilon(k) = \frac{k^2}{2m_B^*} - V_0, \qquad k < k_F, \tag{2.18}$$

where m_B^* and V_0 are determined self-consistently. For the particle spectrum we used kinetic energies, the so-called "standard" choice. Although the HM2Δ contains a weaker tensor force the binding energy calculated for nuclear matter is about the same as the result for the Reid soft core [19]). This is because of the quenching of the bare NN interaction V in the nuclear medium, due to the explicit treatment of isobar degrees of freedom in HM2Δ. This feature seems to be reflected also in the smaller Landau parameters which are obtained for the HM2Δ, see sect. 3.

To calculate Landau parameters from a bare G-matrix it is necessary to make a connection to the formalism discussed in the previous subsection. First we note that instead of using the bare interaction V we must use now the energy-dependent G-matrix in a perturbation series expansion. The energy dependence of the G-matrix is due to its time structure, it is no longer static like the bare Reid soft core for example. In addition the G-matrix, as far as its analytical structure is concerned, has poles in the lower half-plane (particle poles). This is important when energy integrations are performed. Secondly the single-particle Green function now has a self-energy insertion for the hole part. Since one only calculates on-shell self-energy insertions for holes in Brueckner theory, we will simply use a real m^* spectrum for holes. The choice of m^* will be discussed below. Next we note that in the development in subsect. 2.1 one essentially makes use of the fact that the single-particle spectrum is continuous across the Fermi surface [see for example eq. (2.3)]. Therefore we will simply use in further calculations the same m^* spectrum for particles as for holes which clearly preserves this continuity. In doing this we are admittedly not completely consistent and a calculation of the G-matrix with a continuous spectrum as advocated by the Liège group [26]), would shed light on this point. However, we still think that we have taken into account most of the effect of two-body short-range correlations by our procedure while at the same time we can adequately deal with calculations which are sensitive to particle–hole excitation energies. Thus our approximation of the single-particle propagator simply consists of a free single-particle propagator

$$g(k)=\frac{\theta(|\boldsymbol{k}|-k_{\mathrm{F}})}{k_0-\varepsilon(\boldsymbol{k})+i\eta}+\frac{\theta(k_{\mathrm{F}}-|\boldsymbol{k}|)}{k_0-\varepsilon(\boldsymbol{k})-i\eta}, \tag{2.19}$$

with

$$\varepsilon(\boldsymbol{k})=\frac{k^2}{2m^*}-U_0, \tag{2.20}$$

and θ is the step function. Note that $z_{k_{\mathrm{F}}}$ in this approximation is equal to one.

Now we are in a position to relate the G-matrix to the quantities discussed in subsect. 2.1. In a first step we will approximate $\Gamma^{(1)}$ with G [see eq. (2.2)]. Clearly G fulfills the requirements made on $\Gamma^{(1)}$. Then we can obtain the quasiparticle interaction eq. (2.7) by solving the integral equation (2.4). Note that g^2 enters under the integral in eq. (2.4), this means that only hole–hole or particle–particle intermediate states contribute. Performing the energy integration we see that the particle–particle contribution is identically zero due to the analytical structure of the G-matrix discussed above. But at the same time a contribution survives from hole–hole intermediate states due to the energy dependence of the G-matrix. In a time representation this contribution is represented by diagrams with time overlapping G-matrices, see fig. 4. We will take into account this contribution only approximately as we have done in a previous paper [12]). There we have shown that

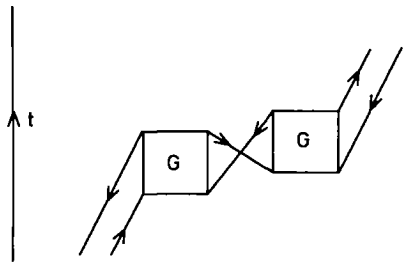

Fig. 4. Contribution to the integral equation (2.4) from hole–hole intermediate states. They arise because the G-matrix has an extended time structure or equivalently is energy dependent.

one can simulate the effect of this contribution quite reasonably choosing a suitable starting energy,

$$E_0 = 2\int_F \frac{d^3p}{(2\pi)^3}\frac{\varepsilon(p)}{\varepsilon(p)-\varepsilon(p-k)}\Big/\int_F \frac{d^3p}{(2\pi)^3}\frac{1}{\varepsilon(p)-\varepsilon(p-k)}. \tag{2.21}$$

Here k is the total hole–hole momentum, note that E_0 is well defined even if $k \to 0$. By taking this choice eq. (2.21) we take into account contributions to Γ^0 as displayed in fig. 4. Our numerical calculations indicate that for some cases this choice has considerable influence on the calculated Landau parameters. This shows that it can be dangerous to relate the G-matrix for a different starting energy to Γ^0 which means neglecting the terms of the kind displayed in fig. 4. The calculation of the Landau parameters proceeds now in a similar way as described in ref. [27]). The results are discussed in sect. 3.

Now we will discuss a second partial summation of diagrams. To make clear what kind of partial summation we would like to make, consider the diagrams in fig. 5. As discussed above diagram 5b, the bare G-matrix, contributes to $\Gamma^{(1)}$ (diagram 5a), but in addition diagrams 5c and 5d contribute. Diagrams 5b, c and d are the first terms of a whole series of diagrams which can be summed in an integral equation.

$$G^c_{\alpha\beta,\gamma\delta}(p,p';k) = G_{\alpha\beta,\gamma\delta}(p,p';k) + \int \frac{d^4q_c}{i(2\pi)^4} G_{\alpha\varepsilon,\eta\delta}(p,q_c;k)g(q_c+\tfrac{1}{2}k)g(q_c-\tfrac{1}{2}k)G^c_{\eta\beta,\gamma\varepsilon}(q_c,p';k), \tag{2.22}$$

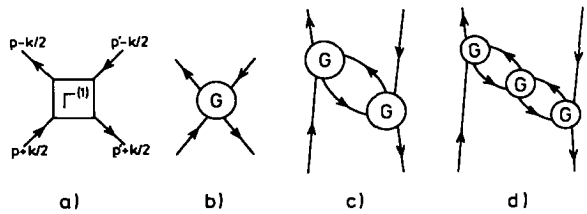

Fig. 5. Diagrams (b), (c) and (d) contribute to the irreducible particle–hole interaction $\Gamma^{(1)}$ [diagram (a)]. Note that diagrams (c) and (d) have no "p-p' cuts" but "k-cuts".

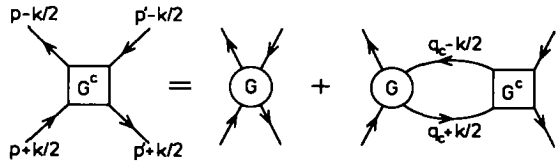

Fig. 6. The integral equation (2.22) we want to study in this paper, since it sums all 'bubble' diagrams in the crossed channel.

which is shown graphically in fig. 6. The renormalized interaction we denote by G^c, where c stands for crossed channel renormalization. The diagrams in fig. 6 are read from left to right and accordingly we arrange the momentum variables in eq. (2.22) in the order incoming, outgoing relative four-momentum and total four-momentum k. The reason why we are interested in summing this special series of diagrams can be pointed out by noting that in the limit $p \to p'$ it is possible to transfer momentum $\boldsymbol{k}$ in the crossed channel in the range $0 \leq \boldsymbol{k} \leq 2k_F$, even when all the external legs are on the Fermi surface, which is the limit of the quasiparticle interaction. This means that when we consider the crossed channel having the quantum numbers corresponding to the pion ($S = 1$, $M_s = 0$, $T = 1$) we are summing the diagrams which lead to pion condensation including also the momentum range where one expects pion condensation. Thus we can argue that it is very important to consider just this type of partial summation. In addition we are able to study the role of the isobars which have been shown to be one of the most important ingredients for pion condensation [1–3]). Also other spin–isospin channels may give rise to similar collective effects which can be studied by summing just these series of diagrams. For the moment we will consider the many-body system to consist only of nucleons. The inclusion of isobar degrees of freedom will be discussed in subsect. 2.3.

We will now develop the integral equation (2.22) to a form which is suitable for numerical calculations and establish the momentum and spin–isospin transformations which are needed to go from crossed channel quantum numbers to the Landau functions [eq. (2.7)]. We will start by developing the momentum transformation. This can be achieved by comparing the different momentum variables given in fig. 7. This gives the following momentum relations

$$\begin{aligned} \boldsymbol{k}_L &= (\boldsymbol{p}+\tfrac{1}{2}\boldsymbol{k})-(\boldsymbol{p}'+\tfrac{1}{2}\boldsymbol{k}) = (\boldsymbol{p}-\tfrac{1}{2}\boldsymbol{k})-(\boldsymbol{p}'-\tfrac{1}{2}\boldsymbol{k}) = \boldsymbol{p}_c-\boldsymbol{p}'_c\,, \\ \boldsymbol{p}_L &= \tfrac{1}{2}\{(\boldsymbol{p}+\tfrac{1}{2}\boldsymbol{k})+(\boldsymbol{p}'+\tfrac{1}{2}\boldsymbol{k})\} = \tfrac{1}{2}(\boldsymbol{p}_c+\boldsymbol{p}'_c+\boldsymbol{k}_c)\,, \\ \boldsymbol{p}'_L &= \tfrac{1}{2}\{(\boldsymbol{p}-\tfrac{1}{2}\boldsymbol{k})+(\boldsymbol{p}'-\tfrac{1}{2}\boldsymbol{k})\} = \tfrac{1}{2}(\boldsymbol{p}_c+\boldsymbol{p}'_c-\boldsymbol{k}_c)\,. \end{aligned} \tag{2.23}$$

We will now establish for which total energy k_0 we will have to solve eq. (2.22). Clearly G^c contains for $k \to 0$ similar poles as Γ in eq. (2.2) for $p \to p'$. Since G^c is contained in $\Gamma^{(1)}$ we see that $\Gamma^{(1)}$ still contains poles for $k \to 0$. However, we are interested only in the limit of all four legs on the Fermi surface and therefore, as

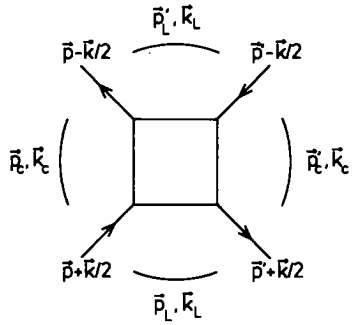

Fig. 7. Momentum variables in Landau and crossed channel. Here p_c, p'_c denote the initial and final relative momentum and k_c the total momentum in the crossed channel, p_L, p'_L and k_L are defined in a similar manner for the Landau channel.

discussed under eq. (2.5), k_0 is strictly zero therefore the limit $k \to 0$ is defined under these circumstances and the singularities do not appear. Now we are in a position to carry out the energy integration in eq. (2.22). Again we obtain a contribution from crossed channel hole–hole intermediate states due to the energy dependence of the G-matrix. However, taking again a suitable starting energy we can simulate this effect and do not have to consider hole–hole states explicitly [see eq. (2.21) and the discussion there]. At the same time we make use of the fact that in actual numerical calculations the contributions from non-diagonal total spin projection channels appeared to be essentially zero; therefore we will omit spin–isospin indices in the following because they can be considered as conserved along the crossed channel. Dropping all superfluous variables we then arrive at

$$G^c(\boldsymbol{p}, \boldsymbol{p}'; \boldsymbol{k}) = G(\boldsymbol{p}, \boldsymbol{p}'; \boldsymbol{k}) + \int_R \frac{d^3 q_c}{(2\pi)^3} \left\{ \frac{G(\boldsymbol{p}, \boldsymbol{q}_c - \tfrac{1}{2}\boldsymbol{k}; \boldsymbol{k}) G^c(\boldsymbol{q}_c - \tfrac{1}{2}\boldsymbol{k}, \boldsymbol{p}'; \boldsymbol{k})}{\varepsilon(\boldsymbol{q}_c) - \varepsilon(\boldsymbol{q}_c - \boldsymbol{k})} \right.$$
$$\left. + \frac{G(\boldsymbol{p}, U(\boldsymbol{q}_c - \tfrac{1}{2}\boldsymbol{k}); \boldsymbol{k}) G^c(U(\boldsymbol{q}_c - \tfrac{1}{2}\boldsymbol{k}), \boldsymbol{p}'; \boldsymbol{k})}{\varepsilon(\boldsymbol{q}_c) - \varepsilon(\boldsymbol{q}_c - \boldsymbol{k})} \right\}. \tag{2.24}$$

Here the operation U is defined as

$$U(\boldsymbol{p}) \equiv U(p, \theta, \phi) = (p, \pi - \theta, \phi) \tag{2.25}$$

and the region R is given in fig. 8, see also ref. [12]). Defining

$$\bar{G}^c(\boldsymbol{p}, \boldsymbol{p}'; \boldsymbol{k}) = \tfrac{1}{2}[G^c(\boldsymbol{p} - \tfrac{1}{2}\boldsymbol{k}, \boldsymbol{p}' - \tfrac{1}{2}\boldsymbol{k}; \boldsymbol{k}) + G^c(U(\boldsymbol{p} - \tfrac{1}{2}\boldsymbol{k}), \boldsymbol{p}' - \tfrac{1}{2}\boldsymbol{k}; \boldsymbol{k}) \tag{2.26}$$

and the analogous definition of $\bar{G}$ we arrive at the integral equation

$$\bar{G}^c(\boldsymbol{p}, \boldsymbol{p}', \boldsymbol{k}) = \bar{G}(\boldsymbol{p}, \boldsymbol{p}'; \boldsymbol{k}) + \int_R \frac{d^3 q_c}{(2\pi)^3} \frac{\bar{G}(\boldsymbol{p}, \boldsymbol{q}_c; \boldsymbol{k}) \bar{G}^c(\boldsymbol{q}_c, \boldsymbol{p}'; \boldsymbol{k})}{\varepsilon(\boldsymbol{q}_c) - \varepsilon(\boldsymbol{q}_c - \boldsymbol{k})}, \tag{2.27}$$

where we have made use of symmetry properties of the G-matrix which were derived in the appendix A of ref. [12]). We see that we obtain an integral equation for the sum

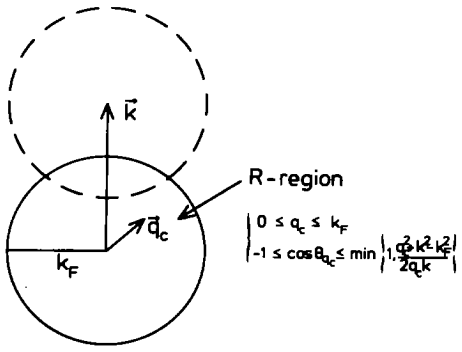

Fig. 8. The space for momentum integration in the integral equation (2.24)

of the matrix elements $G^c(p-\frac{1}{2}k, p'-\frac{1}{2}k; k)$ and $G^c(U(p-\frac{1}{2}k), p-\frac{1}{2}k; k)$. To see which point of region R contributes to the Landau limit we will make use of the transformation given in eq. (2.23). We see that $k_L = 0$ implies $p = p'$ for the first matrix element, the other two relations imply

$$\begin{aligned} p_L &= p\,, \\ p'_L &= p-k\,. \end{aligned} \tag{2.28}$$

This means $|p| = k_F$ and $|p-k| = k_F$, therefore $\cos\theta_p = |k|/2k_F$. With this knowledge one can easily show that $\cos\theta_{p-k/2} = 0$ as well as $\cos\theta_{U(p-k/2)} = 0$. Thus in the Landau limit definition (2.26) sums two equal diagonal matrix elements with relative momentum defined by $|p-\frac{1}{2}k| = [k_F^2 - \frac{1}{4}k^2]^{1/2}$ and $\cos\theta_{p-k/2} = 0$. Finally the Landau angle is given by [see eq. (2.28)]

$$\cos\theta_L = \frac{p_L \cdot p'_L}{k_F^2} = \frac{p^2 - |p|\,|k|\cos\theta_p}{k_F^2} = 1 - \frac{k^2}{2k_F^2}\,. \tag{2.29}$$

The three-dimensional integral equation (2.27) can be decoupled into independent two-dimensional integral equations. For this purpose we define, restoring spin quantum numbers,

$$\begin{aligned} &\bar{G}^{c(n)}_{SM_S,SM'_S}(|p|\theta_p, |p'|\theta_{p'}; k) \\ &\quad = \int_0^{4\pi} \frac{d(\phi_p - \phi_{p'})}{4\pi}\, e^{in(\phi_p-\phi_{p'})/2}\, e^{iM_S\phi_p} \bar{G}^c_{SM_S,SM'_S}(p, p'; k)\, e^{-iM'_S\phi_{p'}}\,, \end{aligned} \tag{2.30}$$

where it is understood that α, δ couple to SM_S and β, γ to SM'_S [see eq. (2.22)]. In appendix A of ref. [12]) it has been shown that n is a conserved quantum number,

which means that for every n we have to solve the integral equation

$$\bar{G}^{c(n)}_{SDM_S,SM'_S}(|p|\theta_p, |p'|\theta_{p'}; k)$$

$$= \bar{G}^{(n)}_{SM_S,SM'_S}(|p|\theta_p, |p|\theta_{p'}; k) + \sum_{M''_S} \int_R \frac{dq_c q_c^2 \, d(\cos\theta q_c)}{4\pi^2}$$

$$\times \frac{\bar{G}^{(n)}_{SM_S,SM''_S}(|p|\theta_p, |q_c|\theta_{q_c}; k)\bar{G}^{c(n)}_{SM''_S,SM'_S}(|q_c|\theta_{q_c}, |p'|\theta_{p'}; k)}{\varepsilon(q_c) - \varepsilon(q_c - k)}, \tag{2.31}$$

with the restrictions

$$\left.\begin{aligned} &n + M_S + M'_S \\ &n + M_S + M''_S \\ &n + M''_S + M'_S \end{aligned}\right\} \text{ even} \tag{2.32}$$

which can be obtained from symmetry properties of the interactions as shown in ref. [12]). Due to these relations the $M_S = 0$ channel is diagonal, it can only couple to $M_S = 0$. The $M_S = 1$ channel can couple to itself but also to $M_S = -1$, however the contribution of this non-diagonal channel appeared to be negligible when numerical calculations were performed. Therefore we are left with six independent spin–isospin channels. The next question to address is the convergence of the expansion (2.30). The best way to show that the convergence is fast, is to consider the partial wave expansion of the matrix elements $G_{SM_S,SM_S}(p, p'; k)$. One can easily show that conservation of n in this case is equivalent with conservation of the projection of the total particle–hole angular momentum M, because performing the integration (2.30) in this representation yields $M = -\frac{1}{2}n$. Therefore, if for example $M_S = 0$, we see that for the $n = 0$ channel we get a contribution from every $LL'J$ particle–hole channel, while for $n = |2|$ a contribution from $J = 0$ is excluded; for $n = |4|$, $J = 0$ and 1 are excluded and so on. Since we can expect also some sort of decrease in the importance of higher partial wave channels due to the short-range nature of the interaction, we may expect that the convergence in n is very good. Indeed the numerical calculations support this conclusion. As we have seen above the point in R which contributes to the Landau limit is defined by the length and the polar angle with respect to k of the relative momentum. Therefore this contribution is independent of ϕ_p and $\phi_{p'}$. Taking these angles as zero we can obtain $\bar{G}^c_{SM_S,SM_S}(p, p'; k)$ from the inverse of eq. (2.30) with the result

$$\bar{G}^c_{SM_S,SM_S}(p, p'; k) = \sum_n \bar{G}^{c(n)}_{SM_S,SM_S}(|p|\theta_p, |p'|\theta_{p'}; k), \phi_p = \phi'_p = 0, \tag{2.33}$$

and analogously for $\bar{G}$.

The actual calculation runs now as follows. We solve the Bethe–Goldstone equation in the particle–particle $LL'SJ$ representation. From these matrix elements one can obtain the Landau functions [eq. (2.7)] and calculate Landau parameters in a

similar way as in ref. [27]). Next for the crossed channel calculation we have to perform a particle–hole transformation which is described in detail in the appendix of ref. [12]). Then one can calculate the n-channel amplitudes and solve the integral equation (2.31). To get the renormalization of the Landau functions due to the crossed channel renormalisation we have added the difference of the renormalized and the bare G-matrix n-amplitudes to the Landau functions of the bare G-matrix. This procedure requires then only the calculation for 3 or 4 n-channels since we found in our numerical calculation that the difference of the renormalized and bare G-matrix n-amplitudes vanishes for higher n-channels. Clearly the six crossed channel spin–isospin amplitudes contribute in a different way to the Landau functions. To show this explicitly we give here the spin–isospin recoupling matrix which relates the Landau functions to the crossed channel amplitudes. It can be obtained by simple recoupling techniques. For clarity we omit the momentum variables which are related to each other by eq. (2.23).

$$
\begin{aligned}
f &= -\tfrac{1}{16}[G^c(0,0,0)+3\,G^c(0,0,1)+2G^c(1,1,0)+\ G^c(1,0,0)+6G^c(1,1,1)+3G^c(1,0,1)],\\
f' &= -\tfrac{1}{16}[G^c(0,0,0)-\ G^c(0,0,1)+2G^c(1,1,0)+\ G^c(1,0,0)-2G^c(1,1,1)-\ G^c(1,0,1)],\\
g &= -\tfrac{1}{16}[G^c(0,0,0)+3G^c(0,0,1)-\tfrac{2}{3}G^c(1,1,0)-\tfrac{1}{3}G^c(1,0,0)-2G^c(1,1,1)-\ G^c(1,0,1)]\\
g' &= -\tfrac{1}{16}[G^c(0,0,0)-\ G^c(0,0,1)-\tfrac{2}{3}G^c(1,1,0)-\tfrac{1}{3}G^c(1,0,0)+\tfrac{2}{3}G^c(1,1,1)+\tfrac{1}{3}G^c(1,0,1)],\\
(\bar{k}/k_F)^2 h &= -\tfrac{1}{48}[\qquad\qquad -2G^c(1,1,0)+2G^c(1,0,0)-6G^c(1,1,1)+6G^c(1,0,1)],\\
(\bar{k}/k_F)^2 h' &= -\tfrac{1}{48}[\qquad\qquad -2G^c(1,1,0)+2G^c(1,0,0)+2G^c(1,1,1)-2G^c(1,0,1)],
\end{aligned}
\tag{2.34}
$$

where we have used the notation $G^c(S, M_S, T)$. Note that spin projection $M_S = 1$ gives the same contribution as $M_S = -1$ (time-reversal invariance). Therefore we consider only $M_S = 1$ and multiply its contribution by a factor 2 in eq. (2.34). The vector $\bar{k}$ is defined as $\frac{1}{2}(p_L - p'_L)$, which is equal to $\frac{1}{2}k$ [see eq. (2.28)] therefore we define the spin quantization axis to lie in the k-direction. In this way we are consistent with the calculation of the H and H' parameters as reported in ref. [27]).

2.3. THE INCLUSION OF ISOBAR CONFIGURATIONS IN THE CALCULATION OF LANDAU PARAMETERS

In this paper we are not interested in defining a quasiparticle interaction in which one or two of the particles are replaced by a Δ-isobar. Instead we are interested in the influence of crossed channel isobar configurations on the Landau parameters of the nucleon–nucleon interaction, because, as we have shown in the preceding subsection, large momenta ($2k_F$) can be transferred in the crossed channel and therefore isobar excitations may be important. From the work on pion condensation [1–3]) we know that it is crucial to consider isobar configurations in the pion channel. Therefore we will study their effect on the crossed channel renormalization discussed in subsect. 2.2. Diagrammatically the coupling of the isobar–nucleon-hole states to the nucleon particle-hole states is shown in fig. 9. Since one also has to take into

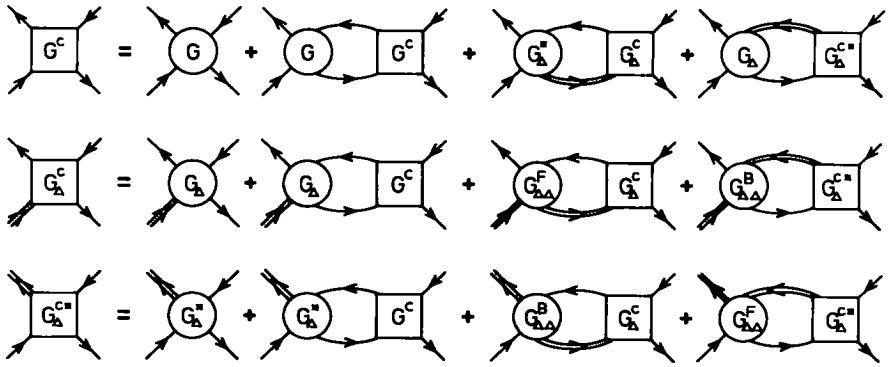

Fig. 9. Coupled set of integral equations [eq. (2.25)] to calculate the crossed channel renormalization with inclusion of isobars.

account the possibility of isobar–nucleon-hole states coupling back to nucleon particle-hole states one has to solve the following set of coupled integral equations

$$G^{c}(p,p';k)=G(p,p';k)+\int\frac{d^4q_c}{i(2\pi)^4}G(p,q_c;k)g(q_c+\tfrac{1}{2}k)g(q_c-\tfrac{1}{2}k)G^{c}(q_c,p';k)$$
$$+\int\frac{d^4q_c}{i(2\pi)^4}G^{*}_{\Delta}(p,q_c;k)g_{\Delta}(q_c+\tfrac{1}{2}k)g(q_c-\tfrac{1}{2}k)G^{c}_{\Delta}(q_cp';k)$$
$$+\int\frac{d^4q_c}{i(2\pi)^4}G_{\Delta}(p,q_c;k)g(q_c+\tfrac{1}{2}k)g_{\Delta}(q_c-\tfrac{1}{2}k)G^{c*}_{\Delta}(q_c,p';k)\,, \qquad (2.35a)$$

$$G^{c}_{\Delta}(p,p';k)=G_{\Delta}(p,p';k)+\int\frac{d^4q_c}{i(2\pi)^4}G_{\Delta}(p,q_c;k)g(q_c+\tfrac{1}{2}k)g(q_c-\tfrac{1}{2}k)G^{c}(q_c,p';k)$$
$$+\int\frac{d^4q_c}{i(2\pi)^4}G^{F}_{\Delta\Delta}(p,q_c;k)g_{\Delta}(q_c+\tfrac{1}{2}k)g(q_c-\tfrac{1}{2}k)G^{c}_{\Delta}(q_c,p';k)$$
$$+\int\frac{d^4q_c}{i(2\pi)^4}G^{B}_{\Delta\Delta}(p,q_c;k)g(q_c+\tfrac{1}{2}k)g_{\Delta}(q_c-\tfrac{1}{2}k)G^{c*}_{\Delta}(q_c,p';k)\,, \qquad (2.35b)$$

$$G^{c*}_{\Delta}(p,p';k)=G^{*}_{\Delta}(p,p';k)+\int\frac{d^4q_c}{i(2\pi)^4}G^{*}_{\Delta}(p,q_c;k)g(q_c+\tfrac{1}{2}k)g(q_c-\tfrac{1}{2}k)G^{c}(q_c,p';k)$$
$$+\int\frac{d^4q_c}{i(2\pi)^4}G^{B}_{\Delta\Delta}(p,q_c;k)g_{\Delta}(q_c+\tfrac{1}{2}k)g(q_c-\tfrac{1}{2}k)G^{c}_{\Delta}(q_c,p';k)$$
$$+\int\frac{d^4q_c}{i(2\pi)^4}G^{F}_{\Delta\Delta}(p,q_c;k)g(q_c+\tfrac{1}{2}k)g_{\Delta}(q_c-\tfrac{1}{2}k)G^{c*}_{\Delta}(q_c,p';k)\,. \qquad (2.35c)$$

Here eq. (2.35a), keeping the first two terms on the r.h.s. only, corresponds to eq. (2.22) which has been discussed above when only nucleon particle-hole states were considered. We have suppressed spin–isospin indices because the calculations have shown that numerically they can be regarded as conserved quantities. The interaction blocks G_Δ and G_Δ^* represent transition potentials converting a nucleon particle-hole state into an isobar–nucleon-hole state and the reverse process, respectively. We have considered π, ρ-exchange transition potentials as in ref. [12]), where we have shown that the influence of short-range correlations on these transitions can be neglected. The blocks $G_{\Delta\Delta}^{\mathrm{F}}$ and $G_{\Delta\Delta}^{\mathrm{B}}$ connect isobar–nucleon–hole states with each other, the difference between the two blocks lies in the time structure; $G_{\Delta\Delta}^{\mathrm{F}}$ represents the interaction which creates and destroys an isobar–nucleon-hole state, while $G_{\Delta\Delta}^{\mathrm{B}}$ creates or destroys two isobar–nucleon–hole states. Again we have used π,ρ-exchange transition potentials and in this case short-range correlations do play an important role so we took them into account as in ref. [12]). Further details on these transition potentials and the necessary particle–hole transformations can be found in ref. [12]). For the isobar single-particle propagator we take

$$g_\Delta(k)=\frac{1}{k_0-\varepsilon^\Delta(\boldsymbol{k})-\omega_\Delta+i\eta}, \tag{2.36}$$

where ω_Δ is the mass difference between an isobar and a nucleon, ε^Δ represents the single-particle spectrum of the isobar which we take purely kinetic for reasons given in ref. [12]). Treating the energy dependence of the G-matrix as in subsect. 2.2 and neglecting the energy dependence of the other interaction blocks we can perform the energy integration in eq. (2.35). Defining analogously to eq. (2.26)

$$\bar{G}_\Delta^{\mathrm{c}}(\boldsymbol{p},\boldsymbol{p}';\boldsymbol{k})=\tfrac{1}{2}[G_\Delta^{\mathrm{c}*}(\boldsymbol{p}-\tfrac{1}{2}\boldsymbol{k},\boldsymbol{p}'-\tfrac{1}{2}\boldsymbol{k};\boldsymbol{k})+G_\Delta^{\mathrm{c}}(U(\boldsymbol{p}-\tfrac{1}{2}\boldsymbol{k}),\boldsymbol{p}'-\tfrac{1}{2}\boldsymbol{k};\boldsymbol{k})], \tag{2.37a}$$

$$\bar{G}_{\Delta\Delta}(\boldsymbol{p},\boldsymbol{p}';\boldsymbol{k})=\tfrac{1}{2}[G_{\Delta\Delta}^{\mathrm{F}}(\boldsymbol{p}-\tfrac{1}{2}\boldsymbol{k},\boldsymbol{p}'-\tfrac{1}{2}\boldsymbol{k};\boldsymbol{k})+G_{\Delta\Delta}^{\mathrm{B}}(U(\boldsymbol{p}-\tfrac{1}{2}\boldsymbol{k}),\boldsymbol{p}'-\tfrac{1}{2}\boldsymbol{k};\boldsymbol{k})], \tag{2.37b}$$

with a similar definition for $\bar{G}_\Delta$ as in eq. (2.37a), we obtain two coupled integral equations

$$\begin{aligned}
\bar{G}^{\mathrm{c}}(\boldsymbol{p},\boldsymbol{p}';\boldsymbol{k})&=\bar{G}(\boldsymbol{p},\boldsymbol{p}';\boldsymbol{k})+\int_{\mathrm{R}}\frac{\mathrm{d}^3q_{\mathrm{c}}}{(2\pi)^3}\frac{\bar{G}(\boldsymbol{p},\boldsymbol{q}_{\mathrm{c}};\boldsymbol{k})\bar{G}^{\mathrm{c}}(\boldsymbol{q}_{\mathrm{c}},\boldsymbol{p}';\boldsymbol{k})}{\varepsilon(q_{\mathrm{c}})-\varepsilon(\boldsymbol{q}_{\mathrm{c}}-\boldsymbol{k})}\\
&\quad+\int_{\mathrm{F}}\frac{\mathrm{d}^3q_{\mathrm{c}}}{(2\pi)^3}\frac{\bar{G}_\Delta(\boldsymbol{p},\boldsymbol{q}_{\mathrm{c}};\boldsymbol{k})\bar{G}_\Delta^{\mathrm{c}}(\boldsymbol{q}_{\mathrm{c}},\boldsymbol{p}';\boldsymbol{k})}{\varepsilon(q_{\mathrm{c}})-\varepsilon^\Delta(\boldsymbol{q}_{\mathrm{c}}-\boldsymbol{k})-\omega_\Delta},\\
\bar{G}_\Delta^{\mathrm{c}}(\boldsymbol{p},\boldsymbol{p}';\boldsymbol{k})&=\bar{G}_\Delta(\boldsymbol{p},\boldsymbol{p}';\boldsymbol{k})+\int_{\mathrm{R}}\frac{\mathrm{d}^3q_{\mathrm{c}}}{(2\pi)^3}\frac{\bar{G}_\Delta(\boldsymbol{p},\boldsymbol{q}_{\mathrm{c}};\boldsymbol{k})\bar{G}^{\mathrm{c}}(\boldsymbol{q}_{\mathrm{c}},\boldsymbol{p}';\boldsymbol{k})}{\varepsilon(q_{\mathrm{c}})-\varepsilon(\boldsymbol{q}_{\mathrm{c}}-\boldsymbol{k})}\\
&\quad+\int_{\mathrm{F}}\frac{\mathrm{d}^3q_{\mathrm{c}}}{(2\pi)^3}\frac{\bar{G}_{\Delta\Delta}(\boldsymbol{p},\boldsymbol{q}_{\mathrm{c}};\boldsymbol{k})\bar{G}_\Delta^{\mathrm{c}}(\boldsymbol{p}_{\mathrm{c}},\boldsymbol{p}';\boldsymbol{k})}{\varepsilon(q_{\mathrm{c}})-\varepsilon^\Delta(\boldsymbol{q}_{\mathrm{c}}-\boldsymbol{k})-\omega_\Delta},
\end{aligned} \tag{2.38}$$

where the phase space for isobar–nucleon-hole states ranges over the whole Fermi

sea F. Using now the same n-channel projection technique as described in subsect. 2.2 one can further reduce this set of three-dimensional integral equations to independent two-dimensional coupled integral equations with good n quantum number. After solving these equations we obtain in a similar manner as in subsect. 2.2 the renormalized contribution to the Landau limit.

3. Results and discussion

3.1. LANDAU PARAMETERS DERIVED FROM BARE G-MATRICES

In the first column of tables 1 and 2 we give the results for Landau parameters calculated from the Reid and the HM2Δ G-matrices, respectively. The starting energy was taken twice the Fermi energy. Some of the Reid parameters have been published before in refs. [23,27]). The slight differences are probably due to the fact that we have supplemented the Reid for higher partial waves ($J>2$) with a one-boson-exchange potential. It should be noted, that the F_0 parameter of the Reid is smaller than -1. This means that the zero sound excitation in nuclear matter would have a lower energy than the ground state. Since, in order to take into account the effect from intermediate hole–hole configurations as displayed in fig. 4, we propose a different starting energy to be used for the calculation of the Landau parameters from a G-matrix, we now turn to column two of tables 1 and 2 where the Landau parameters are shown when the starting energy of the G-matrix is chosen according to eq. (2.21). Notice that the F_0 parameter for the Reid potential becomes larger than -1 restoring the stability with respect to zero sound excitations. We also note that mainly the spin-independent parameters are influenced while the central spin-dependent parameters are much less affected and the tensor parameters are almost insensitive except for modifications due to a different m^*. From these results one can conclude that it is very important to consider the energy dependence of the G-matrix explicitly and thereby to take into account effects from intermediate hole–hole configurations. It should be recalled, that, for the calculation discussed in this paper the Bethe–Goldstone equation has been solved using the standard choice, i.e. pure kinetic energies for the particle–particle state configurations. Using a continuous spectrum also in the Bethe–Goldstone equation [26]) or treating the low-lying particle–particle configurations in a model space calculation with a continuous choice, as done by Poggioli and Jackson [28]), yields an enhancement of the effective mass at the Fermi surface. This enhancement of m^* may partly be counterbalanced by hole–hole configurations as discussed in this paper since they lead to more negative starting energies which means again larger absolute values for the energy denominators in the Bethe–Goldstone equation. On the other hand, a continuous single-particle spectrum in the Bethe–Goldstone equation yields a stronger energy dependence of G which should increase the effects of hole–hole configurations as considered here.

TABLE 1

Landau parameters for the Reid soft-core potential at $k_F = 1.40$ fm^{-1}

	I	II	III	IV
m^*/m	0.603	0.598	0.603	0.588
F_0	−1.012	−0.708	0.072	0.648
F_1	−1.192	−1.205	−1.190	−1.235
F_2	−0.360	−0.343	−0.250	−0.819
F_3	−0.064	−0.067	0.134	−0.025
F_4	−0.058	−0.055	0.087	0.240
F_5	−0.039	−0.040	0.086	0.203
F_6	−0.046	−0.044	0.043	0.057
F'_0	0.377	0.190	0.268	0.036
F'_1	0.363	0.335	0.423	0.494
F'_2	0.102	0.089	0.216	0.394
F'_3	−0.015	−0.014	0.059	0.068
F'_4	0.012	0.010	0.054	0.035
F'_5	−0.001	0.000	0.038	−0.002
F'_6	0.007	0.006	0.053	0.040
G_0	0.340	0.356	0.432	0.165
G_1	0.417	0.423	0.508	0.521
G_2	0.152	0.153	0.256	0.441
G_3	0.045	0.044	0.108	0.158
G_4	0.023	0.023	0.057	0.003
G_5	0.015	0.015	0.042	0.002
G_6	0.012	0.012	0.041	0.035
G'_0	0.814	0.746	0.953	0.994
G'_1	0.017	−0.012	0.034	0.025
G'_2	0.052	0.048	0.120	0.053
G'_3	0.042	0.042	0.129	0.108
G'_4	0.025	0.024	0.079	0.094
G'_5	0.006	0.006	0.061	0.073
G'_6	0.001	0.000	0.047	0.047
H_0	1.517	1.510	1.721	2.497
H_1	2.439	2.420	1.631	1.943
H_2	2.120	2.107	1.031	0.035
H_3	1.631	1.618	0.948	0.029
H_4	1.119	1.111	0.836	0.532
H_5	0.785	0.780	0.756	0.732
H_6	0.517	0.514	0.523	0.546
H'_0	−0.602	−0.602	−0.547	−0.806
H'_1	−0.875	−0.871	−0.409	−0.517
H'_2	−0.813	−0.809	−0.220	0.109
H'_3	−0.614	−0.610	−0.163	0.140
H'_4	−0.439	−0.436	−0.156	−0.057
H'_5	−0.280	−0.278	−0.131	−0.126
H'_6	−0.174	−0.173	−0.092	−0.102

The Landau parameters are defined according to eq. (2.9). The different columns contain results for:

I Bare G-matrix with starting energy equal to $2\varepsilon_F$,

II Bare G-matrix with starting energy taken according to (2.21),

III Crossed renormalized G-matrix,

IV Crossed renormalized G-matrix including isobars.

TABLE 2

Landau parameters for the HM2+Δ potential at $k_F = 1.4\ \mathrm{fm}^{-1}$, for further explanation see table 1

	I	II	III	IV
m^*/m	0.621	0.621	0.664	0.680
F_0	−0.566	−0.387	0.151	0.669
F_1	−1.137	−1.136	−1.008	−0.960
F_2	−0.446	−0.433	−0.415	−0.939
F_3	−0.189	−0.191	−0.136	−0.417
F_4	−0.128	−0.126	−0.062	0.000
F_5	−0.076	−0.078	0.004	0.134
F_6	−0.056	−0.055	0.008	0.081
F'_0	0.465	0.370	0.403	0.241
F'_1	0.415	0.376	0.448	0.435
F'_2	0.179	0.166	0.232	0.409
F'_3	0.074	0.073	0.096	0.191
F'_4	0.045	0.044	0.042	0.021
F'_5	0.026	0.026	0.017	−0.026
F'_6	0.019	0.019	0.021	−0.003
G_0	0.034	0.045	0.058	−0.112
G_1	0.208	0.217	0.332	0.316
G_2	0.116	0.118	0.206	0.383
G_3	0.065	0.065	0.088	0.182
G_4	0.041	0.042	0.028	0.008
G_5	0.027	0.027	0.002	−0.041
G_6	0.018	0.018	−0.002	−0.026
G'_0	0.735	0.697	0.868	0.946
G'_1	0.178	0.158	0.239	0.252
G'_2	0.030	0.025	0.060	0.005
G'_3	−0.008	−0.009	0.010	−0.021
G'_4	−0.011	−0.011	−0.005	0.002
G'_5	−0.009	−0.009	−0.004	0.011
G'_6	−0.005	−0.005	−0.005	0.003
H_0	1.630	1.638	1.825	2.616
H_1	2.725	2.726	2.236	2.691
H_2	2.376	2.379	1.400	0.499
H_3	1.770	1.770	0.898	−0.237
H_4	1.234	1.234	0.682	0.219
H_5	0.832	0.832	0.586	0.757
H_6	0.546	0.547	0.446	0.744
H'_0	−0.623	−0.623	−0.599	−0.862
H'_1	−0.919	−0.920	−0.599	−0.706
H'_2	−0.789	−0.791	−0.247	0.058
H'_3	−0.585	−0.585	−0.088	0.295
H'_4	−0.405	−0.405	−0.043	0.116
H'_5	−0.268	−0.268	−0.045	−0.098
H'_6	−0.171	−0.172	−0.049	−0.146

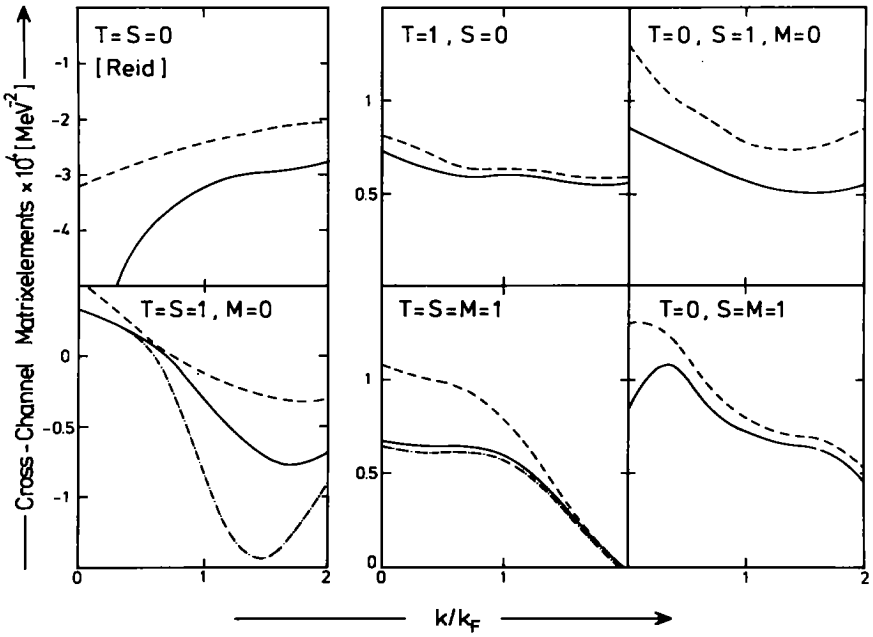

Fig. 10. Crossed channel matrix elements G^c for different spin (S, M_s) and isospin quantum numbers. The momenta have been chosen in such a way that these matrix elements contribute to the Landau limit of the particle–hole interaction. Therefore the matrix elements only depend on the momentum transfer k, which is related to the Landau angle θ_L by eq. (2.29). The dashed curve denotes the result for the bare G-matrix and the solid curve is obtained when the crossed-channel renormalization due to intermediate nucleon particle–hole excitation is taken into account. For the $S = T = 1$ channels the dashed-dotted curve shows the result obtained when isobar configurations are also taken into account. For the results of this figure the Reid potential was used.

3.2. INFLUENCE OF CROSSED CHANNEL RENORMALIZATION

To study the effect of the crossed channel renormalization on the Landau functions, we will first discuss the influence of the integral equation (2.31) on the matrix elements $G^c(S, M_S, T)$ [see eq. (2.34)], which contribute to the Landau limit. The renormalization is different for every spin–isospin crossed channel and the final effect on the Landau functions is given by considering the linear combinations [eq. (2.34)] which describe the transformation from the crossed channel to the Landau channel. In figs. 10 and 11 we have displayed the results for the six spin–isospin channels in the crossed channel for the Reid and the HM2Δ, respectively. In all the figures we show the matrix element which contributes to the Landau limit as a function of the total crossed channel momentum $|k|$, for both the bare and the renormalized G-matrix. Note that $|k|$ is related to the Landau angle θ_L by eq. (2.29). In addition we show for the $S = 1$, $T = 1$ channels the curves when the isobars are included.

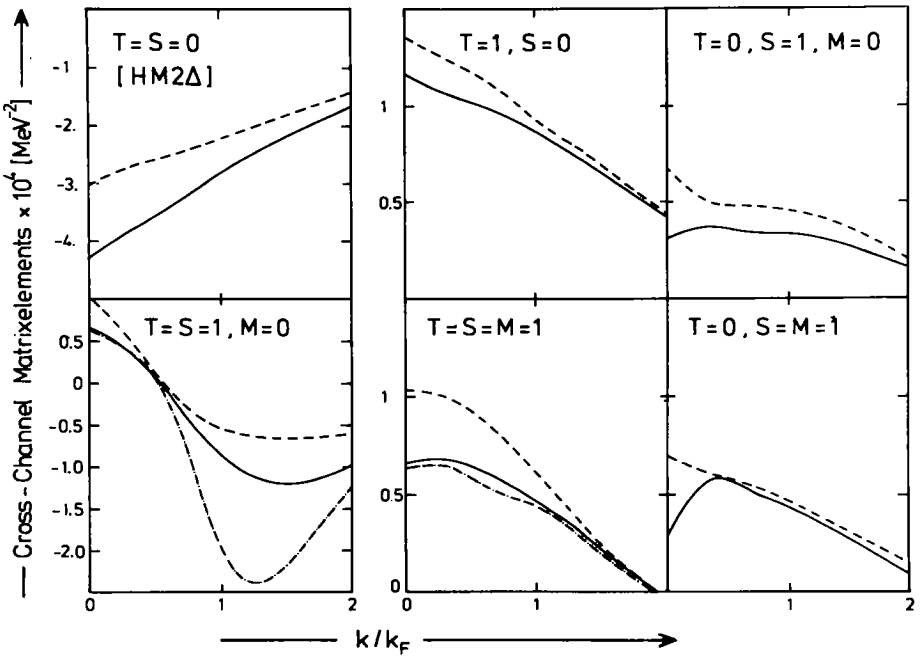

Fig. 11. Crossed channel matrix elements of the HM2Δ potential. For further explanation see fig. 10.

The first thing to note is that the effect of the renormalization always works in the same direction or in other words the difference between a bare matrix element and a renormalized one is positive for all S, M_S, T combinations. This means that repulsive interactions become less repulsive and attractive interactions become more attractive. For both potentials we see that there are only two attractive channels, the $S=0$, $T=0$ and the pion channel ($S=1$, $M_S=0$, $T=1$). Since the bare interactions are sufficiently attractive, large effects show up especially in these channels. Secondly we see that in all channels except the pion channel ($S=1$, $M_S=0$, $T=1$) the renormalization effect decreases when $|k|$ increases, this means that the low momentum transfer region or equivalently the small Landau angle region, is modified especially by these channels. This renormalization for small momentum transfer is mainly due to the crossed channels ($S=T=0$) and ($S=M_S=T=1$). The very strong effect in the pion channel however, is most important for $|k|$ values lying between k_F and $2k_F$, the region of the critical momentum for pion condensation. As we will see later this has important implications for the new Landau parameters. We further note that the influence of the isobars is essentially restricted to the pion channel ($S=1$, $M_S=0$, $T=1$). In the other $S=1$, $T=1$ channel ($M_S=1$) we see hardly any effect. The reason for this is that the attraction of direct one-pion exchange is not operative in the $S=1$, $M_S=1$, $T=1$ channel, therefore one can expect large effects only from direct

ρ-exchange. This, however, starts to be important only for very high $|k|$ which do not contribute to the Landau limit.

To understand how these different renormalizations in the crossed channel contribute to the Landau functions, we have to consider eq. (2.34). As explained in subsect. 2.2 we will need only the difference between the bare and the renormalized G-matrix. This difference can then be added to the original Landau functions to obtain the new ones. The original Landau functions together with the renormalized

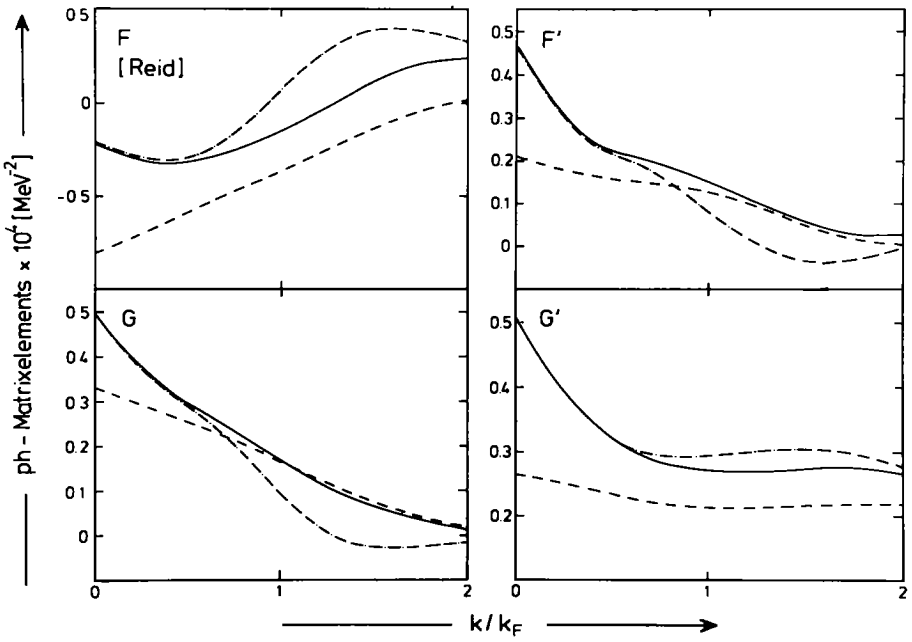

Fig. 12. Particle–hole interaction in the Landau limit as a function of the momentum transfer k. The momentum k is related to the Landau angle θ_L as given in eq. (2.29). The different spin–isospin channels (F, F', G, G') are defined in eq. (2.7). The dashed curve is the result for the bare G-matrix. If the crossed channel renormalization with only nucleon particle–hole excitation is included, the solid line is obtained, whereas the dashed–dotted curve stands for the result with inclusion of isobar configurations. For the NN interaction the Reid soft-core potential has been used.

ones are displayed in figs. 12 and 13. From eq. (2.34) we can conclude that the renormalization for the f-function is coherent. All six crossed channels contribute in the same direction and since the individual contributions of these channels are all positive we see that the crossed channel renormalization will always work in the direction to make f less attractive. This conclusion is different for the other channels since there the contributions add up incoherently. However from an analysis of figs. 10 and 11 together with eq. (2.34) we see that there is always a large identical contribution from the $S=0$, $T=0$ crossed channel to the four central Landau

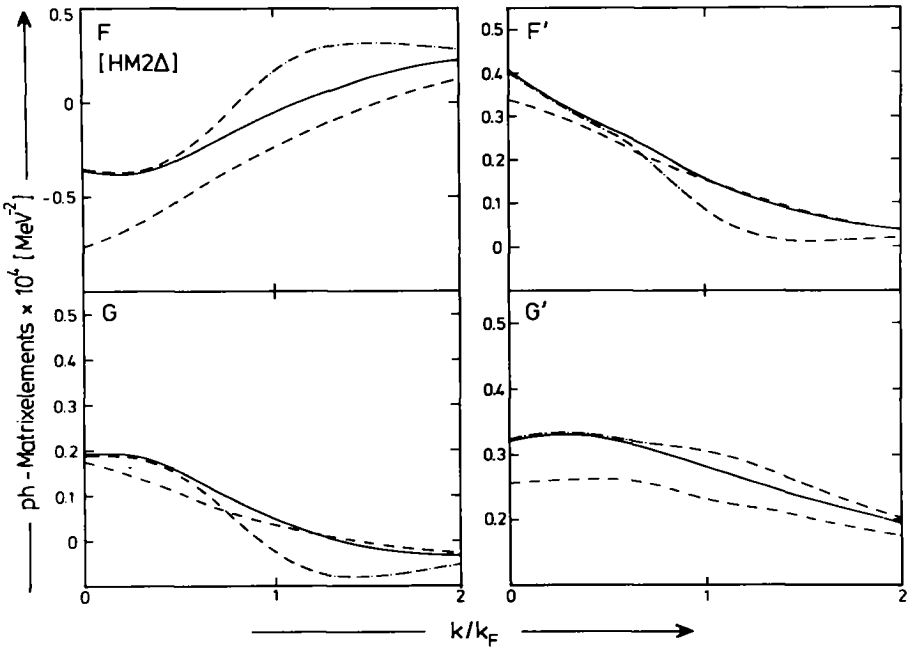

Fig. 13. Particle–hole interaction in the Landau limit for the HM2Δ potential. For further explanation see fig. 12.

functions which tends to make these functions more positive. The other crossed channels contribute with different statistical weight and sign to the Landau functions. Note that the pion channel will make f and g' more positive while f' and g are pushed down by this channel. Although the effect of the pion channel for g' is a factor 9 smaller than for f it still means that collectivity in this channel makes g' larger. Therefore this renormalization of the effective interaction is dynamically opposing the tendency towards pion condensation. Although we have only explicitly considered the Landau limit of the irreducible particle–hole interaction, the same arguments hold for the momentum region in the particle–hole channel which is important for pion condensation. The more the pion crossed channel becomes soft the larger the effect on g', and the more difficult again pion condensation will be.

From figs. 12 and 13 one also can clearly see what enormous influence the introduction of the isobars has (compare the dashed-dotted and the solid lines). To discuss this influence in more detail we will now consider the Landau parameters which are calculated with the inclusion of the renormalization in the crossed channel. These parameters are given in tables 1 and 2. Column three gives the result that the F_0 parameter for the Reid interaction goes from -0.708 to 0.072 for nucleons only while the inclusion of isobars brings this parameter to a value of 0.648. This same sequence for the HM2Δ is -0.387, 0.151 and 0.669. Notice the rather small effect the renormalization has on the effective mass which is related to F_1 by eq. (2.11). The

reason for this unexpected result lies in the contribution of the pion crossed channel. As we have discussed above, the other crossed channels mainly influence the small Landau angles while the pion channel is mainly responsible for changes which occur at larger Landau angles. If we therefore neglect the effect of the pion crossed channel, the f-function would be pushed up only for the lower Landau angles leading to an increase of the effective mass. However it turns out that the inclusion of the crossed pion channel more or less cancels this effect even when isobars are introduced. Only for the MH2Δ do we see a slight increase of the effective mass. The other F-parameters are more strongly influenced. Notice that the contribution of some of the higher F_1 parameters to the sum rules [eqs. (2.16a) and (2.16b)] can be quite large although the importance of these parameters is not yet very clear.

The F' parameters get somewhat less repulsive as compared with the bare G-matrix. For the Reid we see that with isobars F'_0 becomes almost zero which leads to a small symmetry energy [eq. (2.15)], although the small m^* compensates most of the effect. The G-parameters show a similar behaviour. The G_0 for the Reid with isobars becomes much smaller and for the case of HM2Δ G_0 even turns negative. Clearly this effect on the zero-order Landau parameters can be traced back to the very large contribution of the pion crossed channel which according to eq. (2.34) will push up F_0 and G'_0 and make F'_0 and G_0 smaller.

Next we come to the G' parameters. All results show very clearly that the crossed renormalization makes the interaction in the central spin–isospin channel, $g'\sigma_1 \cdot \sigma_2\tau_1 \cdot \tau_2$, more repulsive. It has been discussed already above that this has important consequences for the discussion whether pion condensation occurs in nuclear matter. We also conclude that in this channel only the zero-order parameter really seems to be important. All higher order parameters are rather small. From the calculated Landau parameters one can also deduce values for the compressibility [see eq. (2.14)] and the symmetry energy [eq. (2.15)]. Such values are displayed in tables 3 and 4 for the Reid and the HM2Δ potentials, respectively. The values for the compressibility are enhanced quite drastically with inclusion of the crossed channel renormalization and the resulting values are much higher than the empirical one of

TABLE 3

Compressibility K [eq. (2.14)], symmetry energy β [eq. (2.15)] and sum rules, A and B [left-hand sides of eqs. (2.16a) and (2.16b)] for the Reid soft-core

	II	III	IV
K (MeV)	119	433	683
β (MeV)	27.0	28.5	23.9
A	−3.36	0.55	
B	−4.37	2.95	

The description of the different approximations (II, III, IV) is given in the caption of table 1.

TABLE 4

As table 3 but for the HM2Δ

	II	III	IV
K	241	423	599
β	29.9	28.6	24.7
A	−1.789	−0.481	
B	−2.449	1.291	

about 200–300 MeV [ref. [29])]. It shoud be kept in mind, however, that the present calculation of the compressibility is not performed for the saturation densities of the 2 potentials. Furthermore, since the calculation of the ground state energy requires the full consideration of all 3-body and 4-body terms in Brueckner theory [30]), one may expect that this is also true for the calculation of the compressibility. The calculated symmetry energies are not very sensitive to the crossed channel renormalization and are only slightly reduced. All results agree reasonably well with the empirical value of 25–36 MeV [refs. [31,32])].

Tables 3 and 4 also contain the results for the sum rules (2.16a, b). The deviations from zero indicate to what extent the Pauli principle is violated in the calculated quasiparticle interaction. That it is violated when the quasiparticle interaction is represented by a bare V-interaction or by any iteration like e.g. the G-matrix, which is antisymmetric upon the interchange of ingoing or outgoing lines, has been discussed before [33]). We will briefly show here why the Pauli principle is not obeyed in this case and then show what influence can be expected from the crossed channel diagrams which we have included in our approximation to the quasiparticle interaction. Consider the diagrams in fig. 14 where diagrams a and b represent the first terms which are obtained from iterating eq. (2.5) in the Landau limit. If now we exchange e.g. the incoming lines we obtain diagrams 14c and 14d as exchange diagrams from 14a and 14b, respectively. If now the interaction block is approximated by the G-matrix only, the forward scattering amplitude [eq. (2.5)] contains

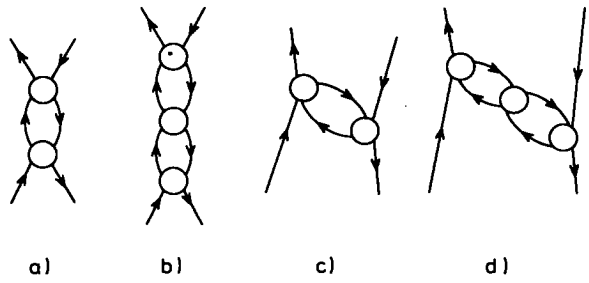

Fig. 14. Diagrams (a) and (b) represent the first terms of a series which is iterated by eq. (2.5) in the Landau limit. When the interaction block is anti-symmetric as in the case of a G-matrix, a corresponding series of exchange with (c) and (d) is missing from the quasiparticle scattering amplitude, therefore the Pauli principle will be violated.

diagrams 14a and 14b but not those of figs. 14c and 14d. Therefore it is not antisymmetric and the sum rules are violated.

There is a whole series of exchange diagrams of type 14c, d missing. This series, however, is just the chain of diagrams which is summed by the crossed channel integral equation (2.22). We may expect therefore that the crossed channel Landau parameters will obey the sum rules better than those of the bare G-matrices. That this is indeed true can be seen from table 3. For both potentials the sum rules are better fulfilled when crossed channel diagrams are included. Still they are not fulfilled exactly because of the following reason: The series which was originally missing and which is indicated in figs 14c, d, is now included. This inclusion, however, yields other, higher order exchange diagrams which are missing now. This is illustrated in fig. 15. Since the upper part of diagram 15a (stands for bare G-interaction) and also the lower part (corresponds to fig. 14c) are now included in our approximation to the quasiparticle interaction, the diagram 15a is contained in the forward scattering amplitude. The exchange term given in fig. 15b, however, is not contained in the forward scattering amplitude. Since the sum rules are obtained from the antisymmetry of the forward scattering amplitude, it is e.g. the omission of diagram 15b which spoils the sum rules in the present approximation.

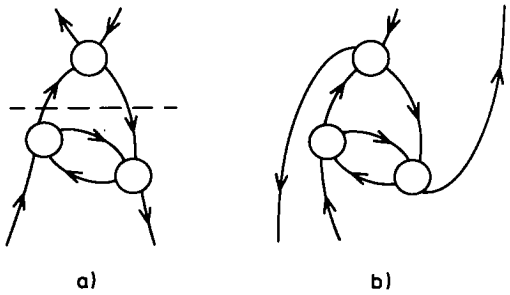

Fig. 15. Diagram (a) is contained in our approximation to the quasiparticle scattering amplitude while diagram (b) is not. Note that we have kept the inner structure of (b) in the same position as compared to (a), to emphasize that only the external lines are exchanged (outgoing lines in this case).

The sum rules (2.16) are derived by only considering nucleon particle–hole states. Therefore it would be inconsistent to apply these sum rules also to the quasiparticle interaction, which takes into account the influence of isobar configurations in the crossed channel. Therefore the corresponding values for A and B are omitted in tables 3 and 4.

At this stage it is useful to compare our method of calculating Landau parameters with the approach developed by Babu and Brown for ^{3}He [ref. [13])] and applied to nuclear matter by Sjöberg [14]). Babu and Brown were able to derive an equation which relates the zero-angle quasiparticle interaction to a so-called direct term and an induced part, which is determined by the quasiparticle interaction itself. This

induced interaction is given by the crossed channel bubble series, containing all terms with at least one bubble. The interaction blocks, however, are given by the quasiparticle interaction itself. Clearly their equation corresponds to the case where both the crossed channel and the Landau channel four-momenta are small. The crucial point now is to extrapolate this equation to crossed channel momenta larger than zero because one also needs the other Landau angles for the determination of the quasiparticle interaction. The extrapolation by Babu and Brown is now performed in such a way that one assumes the interaction for higher crossed channel momenta to be still represented by the Landau functions. Clearly this is a very strong assumption. The advantage of our method lies in the fact that we study the higher crossed channel momenta by using an interaction which is appropriate in this situation, i.e. an interaction which depends on the total crossed channel momentum, as well as the initial and final relative momentum. The importance of this is clearly demonstrated by the fact that in the crossed channel with the pion quantum numbers, the interaction is repulsive for total crossed channel momentum zero while for higher momenta it becomes strongly attractive (see figs. 10 and 11). In addition we are able to study the influence of the isobars explicitly in our approach. With the approximations introduced by Babu and Brown [13]), Sjöberg could iterate the renormalization procedure [14]) and obtained results which fulfill the sum rules if the direct interaction is antisymmetric. The fact that our method still violates the sum rules is in our opinion not such a serious problem: Firstly our results show an important improvement in fulfilling the sum rules when only nucleons are involved and secondly the essential consideration of isobars in the nuclear many-body system will mean that one has to reconsider these sum rules to include the possibility of exciting the isobar degrees of freedom of the nucleon.

To conclude this section we compare our results with the empirical values obtained for finite nuclei [9]). This comparison is given in table 5. The normalization of the Landau parameters is defined in eq. (2.10) using for this table $m^* = m$. Results are

TABLE 5

Landau parameters

		F_0	F_0'	G_0	G_0'
empirical		0.175	0.825	1.438	1.813
Reid	II	−1.184	0.318	0.595	1.247
	III	0.119	0.444	0.716	1.580
	IV	1.102	0.061	0.281	1.690
HM2+Δ	II	−0.623	0.595	0.072	1.121
	III	0.227	0.607	0.088	1.307
	IV	0.958	0.354	−0.165	1.391

Comparison of Landau parameters with the empirical values given in ref. [9]). The normalization is defined according eq. (2.10) using $m^* = m$. For the explanation of the approximations II, III, IV see table 1.

presented for the Reid soft core and the potential HM2Δ. Beside the values for the bare G (approx. II), results for crossed channel renormalization with (IV) and without (III) inclusion of isobar configurations are given. For the comparison with the empirical data one should keep in mind, that the empirical ansatz neglected the influence of tensor channels and only took into account the lowest order term in the Legendre expansion of the Landau functions.

4. Summary and conclusion

In this paper we discuss a microscopic calculation of the quasiparticle interaction in nuclear matter of normal density ($k_F = 1.4$ fm^{-1}). Special attention is paid to the influence of collective features on the quasiparticle interaction. A very prominent example for such a collective feature in nuclear matter is the possibility of pion condensation at a sufficiently high density. If, however, such a collective excitation mode exists, one should also take into account that quasiparticles may interact by the exchange of this collective phonon. It is this effect, the so-called "crossed channel renormalization" which is mainly discussed in this paper.

To perform a microscopic calculation, we start from a Brueckner G-matrix which is derived from two realistic nucleon–nucleon interactions, the Reid soft core [18]) and the HM2Δ potential. Keeping the full complexity of these interactions, which in nuclear matter depend on three momentum variables and the starting energy, the excitation modes for the different spin–isospin channels are evaluated. The influence of the exchange of these phonons on the interaction of quasiparticles at the Fermi surface is investigated by studying the corresponding Landau functions [see eq. (2.7)]. It turns out that the scalar isoscalar mode ($S = T = 0$) in the crossed channel yields strong renormalization for low momentum transfer which means small Landau angle θ_L [see eq. (2.29)]. For large momentum transfer, however, we see a strong renormalization due to the pion channel ($S = T = 1, M_S = 0$). This is due to the strong interaction of the pion with the nuclear medium, which at higher densities may lead to the pion condensate. Since the excitation of isobar states [$\Delta(3, 3)$ resonance] turned out to be crucial for the determination of the threshold conditions for pion condensation [1–3,8,11,12]) they should also influence the size of the crossed channel renormalization. Indeed we see strong effects in our calculations already at normal density (see figs. 10 and 11). Our analysis shows that the results are sensitive to the full momentum dependence of the G-matrix which is used for the renormalization in the crossed channel. Therefore any approximation which neglects this momentum dependence [13,14]) may in general fail to describe the crossed channel renormalization quantitatively.

For the central spin–isospin-independent channel (Landau function f) the renormalizations due to the different crossed channels add up coherently. Therefore there is a strong renormalization for this channel yielding values for the Landau parameter F_0, which are in better agreement with the empirical value [9]) than those obtained for

the bare G-matrix (see table 5). Since for the function F the sum of the renormalization effects from the different crossed channels does not significantly depend on the Landau angle, the Landau parameter F_1, which determines the effective mass m^*, is hardly affected.

A considerable renormalization is also obtained for the Landau parameter G_0'. In a nuclear system which is closer to the threshold for pion condensation, i.e. at higher densities, the renormalization due to the pion crossed channel will be enhanced. This yields a more repulsive value for G_0'. This shows that the crossed channel renormalization tends to prevent pion condensation.

One of us (W.H.D.) would like to thank Prof. Dr. E. Boeker for excellent working conditions at the Vrije Universiteit. Part of this investigation was sponsored by the "Stichting voor Fundamental Onderzoek der Materie (FOM)", which is financially supported by the "Nederlandse Organisatie voor Zuiver Wetenschappelijk Onderzoek (ZWO)". Other parts were supported by the Deutsche Forschungsgemeinschaft.

References

1) G.E. Brown and W. Weise, Phys. Reports **27C** (1976) 1
2) A.B. Migdal, Rev. Mod. Phys. **50** (1978) 107
3) S.-O. Bäckman and W. Weise, in Mesons in nuclei, ed. M. Rho and D.H. Wilkinson (North-Holland, Amsterdam, 1979) p. 1095
4) A.B. Migdal, ZhETF (USSR) **61** (1971) 2210 [JETP (Sov. Phys.) **34** (1972) 1184]; **63** (1972) 1993 [**36** (1973) 1052]
5) R.F. Sawyer, Phys. Rev. Lett. **29** (1972) 382;
D.J. Scalapino, Phys. Rev. Lett. **29** (1972) 386;
R.F. Sawyer and D.J. Scalapino, Phys. Rev. **D7** (1973) 953
6) H. Toki and W. Weise, Phys. Rev. Lett. **42** (1979) 1034
7) J. Delorme, M. Ericson, A. Figureau and N. Giraud, Phys. Lett. **89B** (1980) 327
8) S.-O. Bäckman and W. Weise, Phys. Lett. **55B** (1975) 1
9) J. Speth, E. Werner and W. Wild, Phys. Reports **33C** (1977) 127
10) J. Meyer-ter-Vehn, Phys. Reports, to be published
11) G. Bertsch and M.B. Johnson, Phys. Rev. **D12** (1975) 2230
12) W.H. Dickhoff, A. Faessler, J. Meyer-ter-Vehn and H. Müther, Phys. Rev. **C23** (1981) 1154
13) S. Babu and G.E. Brown, Ann. of Phys. **78** (1973) 1
14) O. Sjöberg, Ann. of Phys. **78** (1973) 39; Nucl. Phys. **A209** (1973) 363
15) G.E. Brown, Proc. Gull Lake Conf. (1979)
16) G.E. Brown, Rev. Mod. Phys. **43** (1971) 1
17) S.-O. Bäckman, Nucl. Phys. **A120** (1968) 593
18) R.V. Reid, Ann. of Phys. **50** (1968) 411
19) K. Holinde and R. Machleidt, Nucl. Phys. **A280** (1977) 429
20) L.D. Landau, ZhETF (USSR) **35** (1958) 95 [JETP (Sov. Phys.) **8** (1959) 70]
21) L.D. Landau, ZhETF (USSR) **30** (1956) 1058 [JETP (Sov. Phys.) **3** (1957) 920]; (USSR) **32** (1957) 59 **5** (1957) 101]
22) A.B. Migdal, Theory of finite Fermi systems and applications to atomic nuclei (Wiley, New York, 1967)
23) J. Dabrowski and P. Haensel, Ann. of Phys. **97** (1976) 452

24) B.L. Friman and A.K. Dhar, Phys. Lett. **85B** (1979) 1
25) M.I. Haftel and F. Tabakin, Nucl. Phys. **A158** (1970) 1
26) J.P. Jeukenne, A. Lejeune and C. Mahaux, Phys. Reports **25C** (1976) 83
27) S.-O. Bäckman, O. Sjöberg and A.D. Jackson, Nucl. Phys. **A321** (1979) 10
28) R.S. Poggioli and A.D. Jackson, Phys. Rev. **C14** (1976) 311
29) J.P. Blaziot, D. Gogny and B. Grammaticos, Nucl. Phys. **A265** (1976) 315
30) B.D. Day, in The meson theory of nuclear forces and nuclear matter ed. D. Schütte, K. Holinde and K. Bleuler (Bibliographisches Institut, Mannheim, 1980)
31) A. Bohr and B.R. Mottelson, Nuclear structure, vol. I (Benjamin, New York, 1969)
32) W.D. Myers and W.J. Swiatecki, Nucl. Phys. **81** (1966) 1; Ann. of Phys. **84** (1974) 186
33) S.-O. Bäckman, Nucl. Phys. **A130** (1969) 427